Directly-Coupled Synchronous Generators With Converter Behavior in Islanded Microgrids

Tine L. Vandoorn, *Student Member, IEEE*, Bart Meersman, *Student Member, IEEE*, Jeroen D. M. De Kooning, *Student Member, IEEE*, and Lieven Vandevelde, *Senior Member, IEEE*

***Abstract*—Because of the increasing share of distributed generation (DG) units, a coordinated approach for their integration in the electrical network is required. Therefore, the microgrid concept has been introduced. Most DG units use power-electronic interfaces, i.e., converters, for which control strategies have been developed such that these units can participate in the microgrid control. Because of the specific characteristics of low-voltage islanded microgrids, such as their resistive nature and lack of inertia, P/V and Q/f droops are often applied for the converter control. However, still some directly-coupled synchronous generators can be present in the microgrid. These generators have different characteristics compared to the converter-based DG units, such as the presence of rotating inertia. Also, their control is mostly based on P/f and Q/V droops. To integrate both synchronous generators and converter-based DG units in an islanded microgrid, their control strategies should be adjusted to each other. As the DG units form the major part of the generators in the islanded microgrid, in this paper, the control of the synchronous generators is changed to introduce converter behavior. The synchronous generators are equipped with P/V and Q/f droop controllers that are adjusted to take the rotating inertia into account. The converter controllers use a variant of P/V droop control to optimize the integration of renewable units in the microgrid.**

***Index Terms*—Converter, distributed generation, droop control, microgrid, synchronous generator.**

I. Introduction

THE grid architecture is changing from centralized to decentralized energy supply with distributed generation (DG) units connected to the utility grid. DG offers many advantages, such as positioning near the consumers which can lead to a reduction of transmission energy losses, an increased usage of environmental friendly resources and postponement of investments in new transmission systems and large-scale generators. Traditional approaches to embed DG focus on minimizing the consequences for the grid performance and safety. However, the rapidly increasing presence of DG units leads to a changed power system operation, with bidirectional power flows in an active distribution network [1]. Hence, the fit-and-forget strategy of installing DG is not a sustainable option and DG will need to cooperate in the grid control and balancing. An approach to deal with the large increase of decentralized, often unpredictable, power sources is the coordinated approach presented by the microgrid [1]–[4]. Microgrids are also likely to play a key role in the evolution of the smart grid [5], [6] as it is expected that the smart grid will emerge as a system of integrated smart microgrids [7]. A key advantage is that the microgrid appears to the power network as a single controllable unit [8]. The intended operation of the microgrid can follow two operating conditions: grid-connected mode and islanded mode. In the grid-connected mode, the DG units in the microgrid support the main grid. The microgrid can be disconnected from the main grid during large disturbances (voltage collapse, faults, poor power quality), feeding only local loads in the islanded mode, which is the focus of this paper. Islanded microgrids can also be applied in remote places where no main grid is available. In this configuration, the microgrid elements are responsible for voltage and power control.

Most DG units are connected to the microgrid via power-electronic interfaces [9], lacking the rotational inertia upon which the conventional grid control is based. Hence, in order to fully exploit the possible advantages of converter-based islanded microgrids, adequate control strategies that are specifically designed for these converters need to be developed. To avoid a critical information infrastructure and single points of failure, that decrease the system reliability, droop-based control is widely used. The P/f droop control method of [10]–[14] is based on the conventional grid control, with P the active power and f the frequency. However, in resistive microgrids, a linkage between active power P and grid voltage V_{g} instead of frequency exists [15]. To take into account this linkage, often the $P/V\mathrm{g}$ droop control strategy is used instead of the P/f droop control [16], [17]. In this paper, a variant of P/V_{g} droop control, namely voltage-based droop control, is used that combines P/V_{g} droop control with $V_{\mathrm{g}}/V_{\mathrm{dc}}$ voltage droops, with V_{dc} the dc link voltage [18]. The voltage level to change the active power depends on the nature of the energy source. In this way, the power changes of the renewable energy sources are delayed compared to those of the dispatchable DG units.

However, when directly-coupled synchronous generators (SGs) are included in this network, their control strategy conflicts with the P/V_{g} droop control and its variants. Generally, the control of the SGs uses the frequency as a parameter to

Manuscript received May 11, 2011; revised August 29, 2011; accepted December 15, 2011. The research was carried out in the frame of the Inter-university Attraction Poles programme IAP-VI-021, funded by the Belgian Government. The work of J. De Kooning was supported by the Special Research Fund (BOF) of Ghent University (Belgium). The work of T. Vandoorn was supported by a Fellowship from FWO. This work was supported by the FWO-Vlaanderen (Research Foundation—Flanders, Belgium).. Paper no. TPWRS-00432-2011.

The authors are with the Electrical Energy Laboratory (EELAB), Department of Electrical Energy, Systems and Automation (EESA), Ghent University, B-9000 Ghent, Belgium (e-mail: Tine.Vandoorn@UGent.be; Bart.Meersman@UGent.be; Jeroen.DeKooning@UGent.be; lieven.vandevelde@UGent.be).

Color versions of one or more of the figures in this paper are available online at http://ieeexplore.ieee.org.

Digital Object Identifier 10.1109/TPWRS.2011.2181544

trigger active power change, while the converter-interfaced distributed generation (CIDG) units have the terminal voltage as the trigger parameter. Also, the presence of the rotating inertia of the SGs must be taken into account. For this, one possibility is to emulate inertia in P/f droop controlled CIDG units, which requires additional storage [19]. However, instead of altering the control of the CIDG units like in [19], in this paper, the control strategy of the SGs is modified to comply with the voltage-based droop control. The reason to change the control strategy of the SGs instead of that of the CIDG units, is that the SGs generally form the minor part of the generators in the microgrid in which mostly a high share of renewable-based, often converter-interfaced, units is present [20]. Converter behavior is included in the SGs, which does not require additional storage in the DG units and is based on the $P/V_{\rm g}$ and Q/f droop control taking into account the rotating inertia of the SG.

In this paper, a brief overview of the control of SGs in conventional networks and CIDG units in microgrids is given. Secondly, the problem of including SGs with conventional control in resistive microgrids is discussed and a new control approach is presented. In the following paragraph, more details about the controllers are given and a basic case is discussed. Finally, two situations are studied: one with an SG in a microgrid and a second one based on the IEEE 13-bus system.

II. Primary Control: Directly-Coupled Synchronous Generators Versus Converter-Interfaced DG Units

In this paragraph, firstly a short overview of the conventional control of SGs to achieve power sharing based on the inertia of the system is given. Secondly, the droop control strategies in microgrids, based on the line parameters, are summarized.

A. Control of Directly-Coupled Synchronous Generators: Conventional Method

The conventional active power control is largely based on the inertia of the SGs that are often large centralized units connected to the transmission network. In case the generators measure an increasing grid frequency, which is proportional with their rotational speed, they conclude that an excess of generated power is present. Therefore, the generators are equipped with a droop mechanism to decrease the mechanical power P_m in case of increasing grid frequency f:

$$P_m = P_{\rm nom} - k_p(f - f_{\rm nom}) \tag{1}$$

with k_p the droop constant and where "nom" denotes nominal values. In this way, a stable system operation is obtained. The frequency changes measured by all generators are the same as the grid frequency is a global parameter.

Because of the inductive nature of the high-voltage networks, the reactive power is mainly determined by the voltage difference. Hence, the generators change their back-emf E based on the measured reactive power. Therefore, for the reactive power sharing, the generators are equipped with a reactive power/voltage droop controller:

$$E = E_{\rm nom} - k_q(Q - Q_{\rm nom}) \tag{2}$$

with k_q the droop constant.

B. Control of Converter-Interfaced DG Units

For the control of the CIDG units in islanded microgrids, communication-based control algorithms, such as master/slave and central control can be used [21]–[24]. The droop control method, on the other hand, does not require communication for the primary control. This is beneficial in terms of reliability and modularity. Therefore, in this paper, only the droop control method is discussed. To include droop control, there are two main paths, namely: droop control based on the inductive or the resistive character of the network lines.

1) Droop Control in Inductive Networks: These droop controllers use an analogous control method as the conventional grid control. Hence, a $Q/V_{\rm g}$ droop controller according to (2) and P/f droops with slope $k_{\rm f}$ are used [1], [10], [13], [17], [25]–[28]:

$$P = P_{\rm nom} - k_{\rm f}(f - f_{\rm nom}). \tag{3}$$

According to the terminal frequency f, this droop controller changes the dc-side power P of the converter [a voltage-source inverter (VSI)], which is analogous to the mechanical input power P_m of conventional SGs. Opposed to P/f droop control of SGs, the P/f droop control of the CIDG units is not based on the rotating inertia of the system. The P/f droop control strategy is applicable because of the linkage between the active power and the phase angle in case of inductive lines, the phase angle dynamically determines the frequency.

2) Droop Control in Resistive Networks: In this paper, low-voltage microgrids are considered in which the microgrid lines are assumed to be mainly resistive. This is a valid assumption because microgrids are low-voltage networks. E.g., a typical R/X value in low voltage lines is 7.7 [17], [29]. Also, a control loop known as the virtual output impedance loop is included to change the output impedance of the converter, to increase the stability of the system and to share linear and nonlinear loads [30]–[32]. In this paper, a resistive output impedance is used in the converter as this provides more damping in the system [15] and complies with the power control strategies of the generators, which are based on the resistive nature of the network.

In networks with resistive lines, a linkage between the active power and the grid voltage; and the reactive power and the phase angle is obtained [15]. Again, changing the phase angle difference is implemented with small changes of frequency. For this purpose, instead of P/f and $Q/V_{\rm g}$ droops, the reversed $P/V_{\rm g}$ and Q/f droops can be implemented in the converters [16], [17]. A variant of this method is the voltage-based droop controller that is depicted in Fig. 1 [18]. The dc-link voltage $V_{\rm dc}$ of the converters dc-bus communicates a difference between the ac-side power (injected into the microgrid) and the dc-side power (delivered by the primary energy source). Therefore, $V_{\rm dc}$ is drooped with the ac-terminal voltage $V_{\rm g}$, according to

$$V_{\rm g} = V_{\rm g,nom} + k_d(V_{\rm dc} - V_{\rm dc,nom}) \tag{4}$$

with k_d the droop parameter. However, in case $V_{\rm g}$ exceeds a certain voltage, the dc-power of the generator is changed by the $P_{\rm dc}/V_{\rm g}$ droop controller:

$$P_{\rm dc} = P_{\rm dc,nom} - k_P(V_{\rm g} - V_{\rm g,nom}). \tag{5}$$

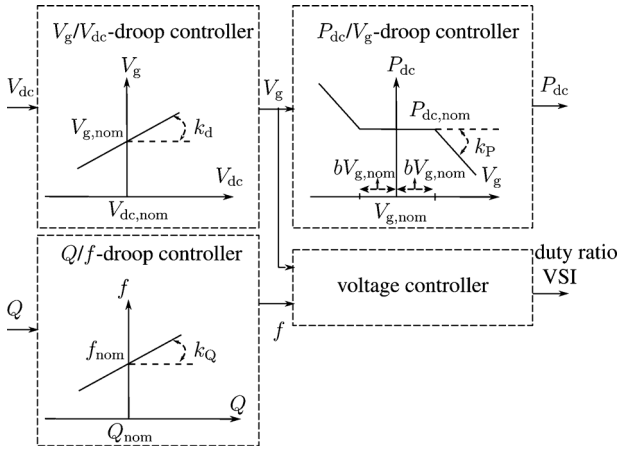

Fig. 1. Active power control in low-voltage microgrids: V_g/V_{dc} droop control.

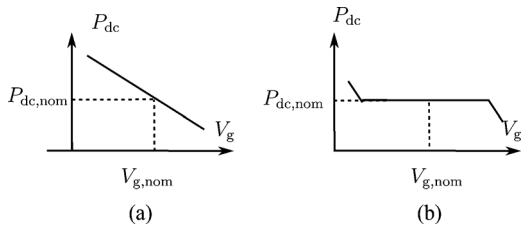

Fig. 2. Dispatchable versus less controllable units (a less controllable unit often uses a renewable source, such as photovoltaic panel, wind turbine or combined heat and power with heat as primary driver). (a) Dispatchable unit. (b) Less controllable unit.

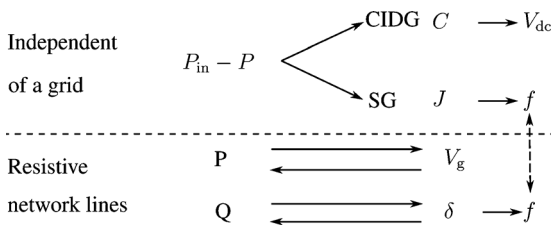

Fig. 3. Energy balance and power flows in resistive networks.

If the grid voltage does not exceed this voltage, the active power remains constant, so this voltage band is called the constant-power band and is defined by

$$V_{g,nom} - V_{g,low} < V_g < V_{g,nom} + V_{g,up} \tag{6}$$

as depicted in Fig. 1. Often, $V_{g,low} = V_{g,up}$, such that in the constant power band

$$(1-b)V_{g,nom} < V_g < (1+b)V_{g,nom} \tag{7}$$

with $2b$ the width of the constant power band. The constant-power band width is dependent on the nature of the energy source, such that b is larger for DG units based on renewable energy sources compared to dispatchable units as depicted in Fig. 2. This enables to delay changing the output power of the renewable sources compared to that of the more dispatchable units. In this way, the method can achieve optimized integration of renewable energy sources in the microgrid.

Analogously to P_{dc}/V_g droop control, I_{dc}/V_g droop control is used in case of current-controlled DG units.

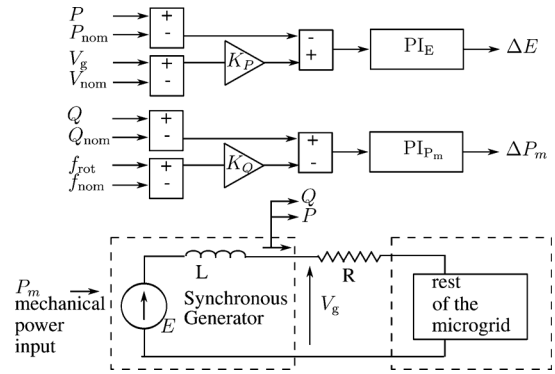

Fig. 4. First order model of synchronous generator in microgrid. PI controllers to control P_m and E. R represents the summation of the stator resistance of the SG and the line resistance of the line between the SG and the rest of the microgrid.

For the reactive power sharing, Q/f droop control is used according to

$$f = f_{nom} + k_Q(Q - Q_{nom}). \tag{8}$$

III. Synchronous Generators in Islanded Microgrids

A. Change of Control Strategy of CIDG Units Versus SGs

The major part of the generators in a microgrid are power-electronically interfaced [9]. However, a small share can be based on directly-coupled SGs with excitation winding. SGs include, for example, diesel generator sets that are widely used as backup or emergency power systems or to electrify remote places. In this paper, with SGs, directly-interfaced SGs are assumed. Converter-interfaced SGs can use the same control strategy as the CIDG units.

Despite the fact that the SGs form the minor part of the generators in the islanded microgrid, they can inject a significant amount of power during some periods (e.g., low sun and wind times). In this paper, the CIDG units use voltage-based droop controllers, while generally, the SGs use a different control strategy. These different control strategies of SGs and CIDG units can pose some problems in the microgrid. In case the SGs use a grid-following control strategy, no conflict arises with the grid-forming CIDG units. However, then, the SGs are current-controlled and inject a pre-specified amount of power while following the grid voltage posed by the CIDG units. Hence, the SGs do not participate in the power sharing according to the ratings of the units of the islanded microgrid. As these units are often dispatchable, opposed to a large share of the CIDG units that can be renewable-based, this is not an optimal situation and does not benefit the stability of the network.

Often , the SGs use a grid-forming strategy, namely the conventional P/f droop control. Hence, e.g., to change the output power, the controllers of the CIDG units (P/V_g) and SGs (P/f) are triggered by different parameters. Subsequently, accurate power sharing is not possible and the stability of the microgrid can be jeopardized. Next to different triggers to change the active power of the units, also active power changes in the network have a different effect on the units as clarified by using

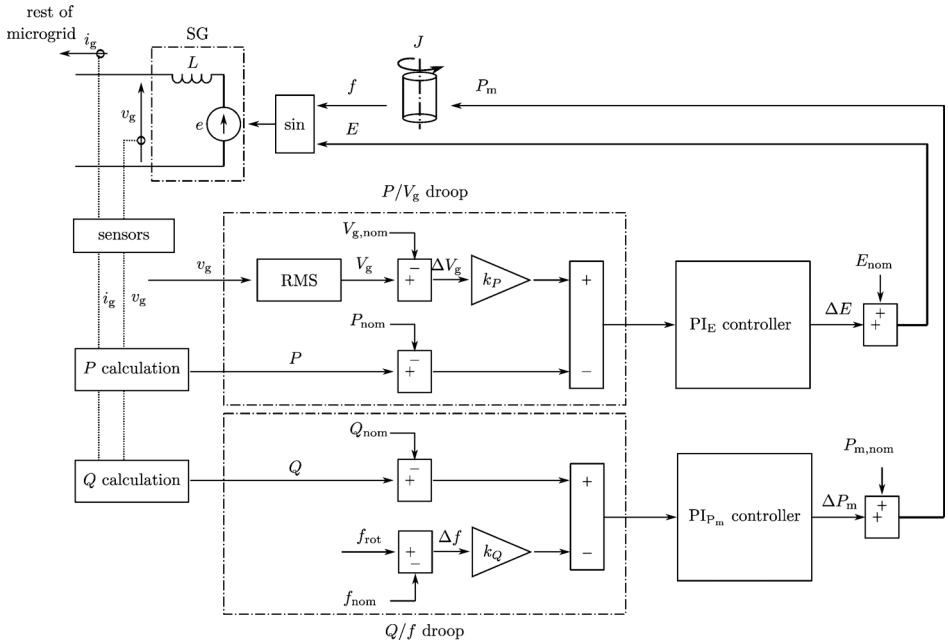

Fig. 5. Overall control of SG unit with voltage-based droop control.

Fig. 3. Firstly, for the CIDG units, in case of an unbalance between dc-power ($P_{\rm dc} = P_{\rm in}$) and delivered ac power P, the dc-bus capacitor absorbs the difference, which changes the dc-bus voltage. The $V_{\rm g}/V_{\rm dc}$ droop controller in turn changes $V_{\rm g}$. For the SGs, a difference between $P_{\rm m}$ ($P_{\rm m} = P_{\rm in}$) and P is absorbed by the rotating inertia J of the generator, changing the terminal frequency. Therefore, active power changes in the network affect the frequency in case of SGs and voltage in case of CIDG units. Also, in case of SGs, frequency changes are induced by active power changes, while in case of CIDG units, the frequency changes are induced by reactive power changes. This leads to an interference between the frequency changes of the units. The same is valid for grid voltage changes.

To avoid this interference, the control strategies of the SGs and CIDG units should be matched to each other for their integration in a resistive islanded microgrid. To match the control of the SGs and the CIDG units, two approaches are possible. In the first approach, the control of the CIDG units is changed. A method for this, known as virtual synchronous generators, is briefly discussed in Section III-C. The approach followed in this paper is to change the control of the SGs as they generally form the minor part of the units in the islanded microgrid, because of the increasing share of inverter-interfaced units [20].

B. Synchronous Generators With Converter Behavior

By changing the control strategy of the SGs to comply with the $P/V_{\rm g}$ droops of the CIDG units, SGs can take part in the active and reactive power sharing in the microgrid. This is studied in this paper, by including $P/V_{\rm g}$ and Q/f droops in the SGs, and as such incorporating SGs with converter behavior in the microgrid.

An SG is, in this paper, modeled by an inductance L in series with a back-emf E as depicted in Fig. 4. As depicted in this figure, two parameters of the SG can be controlled, namely the mechanical power P_m and the back-emf E. The frequency (or phase angle) of the terminal voltage $V_{\rm g}$ can only be controlled indirectly by changing the mechanical (input) power P_m of the SG. The amplitude of $V_{\rm g}$ can be controlled by changing E, which, in turn, is done indirectly by changing the excitation current. The automatic voltage regulator (AVR) of the SG can be used, but the set points are different compared to the conventional control of the AVRs.

Emulating converter behavior, with $P/V_{\rm g}$ and Q/f droop controllers, in SGs is not evident. The main reasons are:

- the presence of rotational inertia. In an SG, when there is an unbalance between the ac-side power P and the input power P_m, the rotational speed of the SG will change. A changed rotational speed will affect the terminal frequency of the SGs. Because of the resistive microgrid lines, this will in turn influence the reactive power output of the generator. Hence, the active and reactive power changes of the SG are linked through the rotational inertia.
- the frequency and phase angle of the output voltage of an SG is more difficult to control compared to that of CIDG units, because the frequency is imposed by the rotational speed of the SG.

To solve this issue, the operating points of the SG are forced towards the $P/V_{\rm g}$ and Q/f droops by controlling E and P_m as depicted in Fig. 5. E is changed to include the $P/V_{\rm g}$ droop control for active power sharing as E and $V_{\rm g}$ only differ through the equivalent inductance of the SG. P_m is changed to use the Q/f droop control to achieve reactive power sharing between multiple SGs and CIDG units as P_m and frequency changes are interdependent through the rotational inertia. Because of the linkage between both, the E and P_m controllers operate with a different bandwidth, avoiding dynamical interactions between the controllers.

To shift the operation towards the $P/V_{\rm g}$ droop, a PI controller is included, operating on the back-emf E of the SG, with $E = E_{\rm nom} + \Delta E$. The input of this PI$_{\rm E}$ controller is

$$-(P - P_{\rm nom}) + k_P(V_{\rm g} - V_{\rm nom}) \tag{9}$$

with $V_{\rm g}$ the rms terminal voltage of the SG, P the ac-side active power and k_P the negative droop parameter. The back-emf E is, in turn, controlled by changing the excitation current of the SG. Because this is fast compared to changing $P_{\rm m}$, the dynamics of this are neglected. The SGs are not equipped with a constant-power band, as generally, these units are dispatchable units in the islanded microgrid.

The frequency f of the back-emf, referred to the stator, is determined by the inertia J of the SG according to

$$P_m - P = \omega J \frac{d\omega}{dt} \tag{10}$$

with $P_{\rm m}$ the input power, P the output ac power of the SG and $\omega = 2\pi f$. In a synchronous generator, the mechanical speed is proportional with the electrical frequency f through the number of pole pairs of the SGs. Here, the electrical speed is considered such that $f_{\rm rot} = f$. Therefore, f can be forced towards the Q/f droop by changing the mechanical power $P_{\rm m}$ of the generator. Generally, $P_{\rm m}$ changes are relatively slow. Hence, a slower $\mathrm{PI}_{\mathrm{P}_m}$ controller with as output $\Delta P_{\rm m}$ is implemented. The input of this PI controller is

$$(Q - Q_{\rm nom}) - k_Q(f_{\rm rot} - f_{\rm nom}) \tag{11}$$

with Q the ac-side power and k_Q the droop parameter. The mechanical power equals $P_m = P_{\rm nom} + \Delta P_m$. If the mechanical power cannot be adjusted fast enough, some storage needs to be included. Except for the slow $\mathrm{PI}_{\mathrm{P}_m}$ controller and some small delay times, the dynamics of changing $P_{\rm m}$ are further neglected because of the small size of the SGs leading to relatively fast possible changes of $P_{\rm m}$ compared to the large central generators.

C. Discussion

Permanent-magnet synchronous machines (PMSMs) are not considered as SGs for two reasons. Firstly, PMSMs often use converter interfaces. Secondly, the reactive power of PMSMs cannot be controlled actively as the excitation field, that determines the back-emf E, can be assumed as largely constant. Therefore, they cannot take part in the reactive power sharing in the microgrid, thus, the Q/f droop controller is not active. For the active power droop, an analogous PI controller as (9) can be included, but with output ΔP_m instead of ΔE. This is out of the scope of this paper.

The P/f droop control method in microgrids is largely based on the inductance of the lines. Hence, the basis for using this control becomes weak in low-voltage, thus resistive, microgrids. This can be solved by adapting the classical P/f droop control method to account for the line impedance by using reference frame transformation [27], [33] or by output impedance design in the virtual output impedance method [34]. However, the smaller the system's rotational inertia, the larger the frequency deviation for a given unbalance between load and mechanical supply. Therefore, in microgrids, that generally have a low total rotating inertia, this may induce large and fast frequency deviations that can make it difficult to overcome problems of frequency instability. On the other hand, power electronics are very flexible and the CIDG units show very fast response compared to the conventional generators. Therefore, CIDG units with P/f droop control are implemented as virtual synchronous generators to contribute to the grid's inertial response in [19], [20], and [35]. For this, the DG units need to reserve a certain percentage of the output power to emulate a source with a certain rotational inertia towards the grid. This requires some additional storage.

IV. Tuning of the Controllers

In this paragraph, the tuning of the PI controllers of the CIDG units and SGs is discussed, taking into account the fast dynamics of the CIDG unit controllers and the slower response of the SGs.

A. Model and Voltage Controllers of the CIDG Units

Fig. 6 shows the summarized overall control strategy of the voltage-based droop control and the cascaded PI voltage control [36]. A single-phase DG unit is considered with an LC filter for the attenuation of switching ripple with $L = 2$ mH, $C = 3$ μF, the switching and sample frequency f_s equal 25 kHz and $V_{\rm dc,nom} = 450$ V. A bridge-type VSI is studied with simulations up to the level of the converter switches. An ideal source from the dc-side is considered, thus, the energy source is not modeled as this does not influence the control strategy. The active and reactive power controllers are based on droops, the tuning of which is already widely discussed as being derived from a tradeoff between gain and stability [37], [38].

The $\mathrm{PI}_{\rm I}$ controller of the inner current control loop in Fig. 7 is tuned by using the transfer function

$$\frac{V_{\rm dc}}{sL} \tag{12}$$

combined with a Pade approximation for delay time ($T_s = 1/f_s$), P, as the PWM control uses discrete time steps with the sample frequency

$$P = \frac{1}{\frac{T_s^3 s^3}{3!} + \frac{T_s^2 s^2}{2!} + T_s s + 1}. \tag{13}$$

The following controller in the z-domain is obtained:

$$\mathrm{PI}_{\rm I} = \frac{0.04594z - 0.0318}{z - 1}. \tag{14}$$

In cascaded PI control, it is important to achieve a fast inner control loop and a slower outer control loop. Therefore, the $\mathrm{PI}_{\rm I}$ controller is tuned primarily according to a desired bandwidth and phase margin, here 1.9 kHz and 30 deg, respectively as depicted in Fig. 8. The PI controller of the outer voltage control loop has a lower bandwidth and is tuned according to

$$\frac{\mathrm{PI}_{\rm I}\frac{V_{\rm dc}}{sL}P}{1 + \mathrm{PI}_{\rm I}\frac{V_{\rm dc}}{sL}P}\frac{1}{sC} \tag{15}$$

with Pade approximation P. Note that the inner current control loop can also be neglected (equivalent transfer function equal to

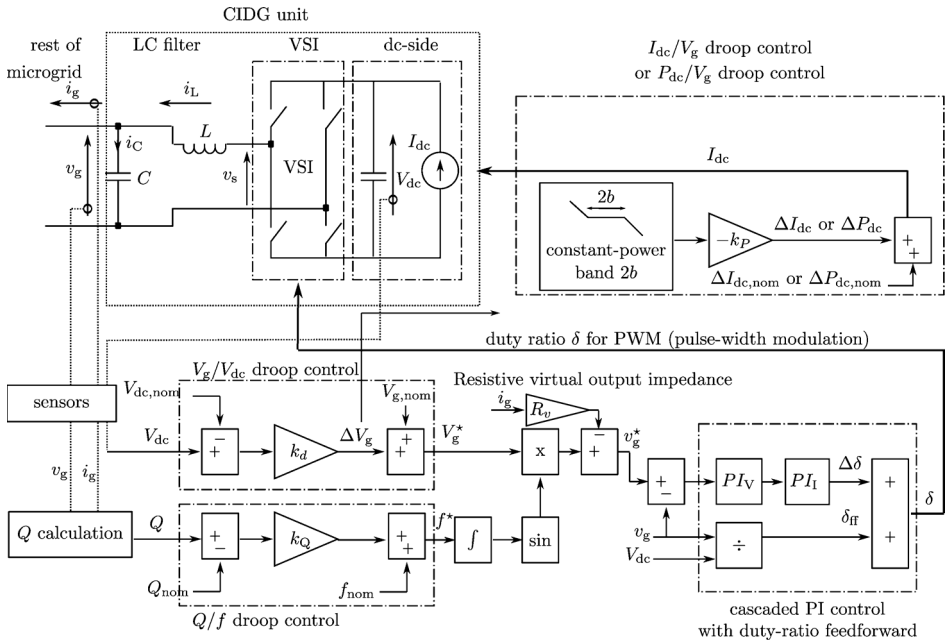

Fig. 6. Overall control of CIDG unit with voltage-based droop control.

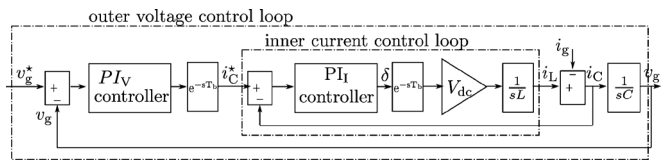

Fig. 7. Tuning voltage control loop CIDG unit: $\mathrm{PI_V}$ is the PI controller in the outer voltage control loop and $\mathrm{PI_I}$ is the PI controller in the inner current control loop.

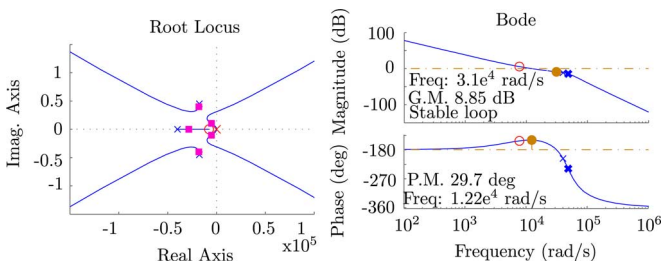

Fig. 8. Root Locus of the $\mathrm{PI_I}$ control loop.

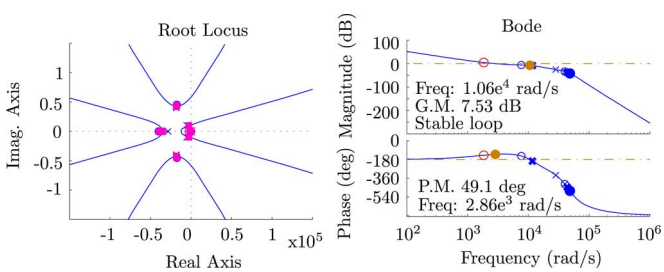

Fig. 9. Root Locus of the $\mathrm{PI_V}$ control loop.

one) in cascade control in case of sufficient different bandwidths of the control loops. The following controller is obtained:

$$\mathrm{PI_V} = \frac{0.006539z - 0.006055}{z - 1} \tag{16}$$

which has a bandwidth of 455 Hz and a phase margin of 49 deg as depicted in Fig. 9.

B. Model and PI Controllers of the SG Voltage-Based Droop Controller

An SG is, in this paper, modeled by an inductance $L = 6$ mH in series with a back-emf E. A single-phase equivalent is considered for a three-phase SG. The $\mathrm{PI_E}$ controller is tuned using the instantaneous power $p(\mathrm{t})$ equation:

$$p(\mathrm{t}) = e(\mathrm{t})i(\mathrm{t}) \tag{17}$$

with $e(\mathrm{t})$ the emf of the SG and $i(t)$ its output current. By using a low-pass filter, the active power can be derived:

$$p = E\frac{E - V}{R + sL}\frac{\omega_c}{s + \omega_c} \tag{18}$$

with $\omega_c = 2\pi 25$ rad/s, V the load voltage and L and R the combined line and SG impedances. In small signal analysis

$$P = \frac{2E_{\mathrm{nom}}\omega_c \Delta E}{(R + sL)(s + \omega_c)} \tag{19}$$

with $E_{\mathrm{nom}} = 250$ V (calculated from $P_{\mathrm{nom}} = 1500$ W, $V_{\mathrm{g,nom}} = 230$ V, $R = 2\ \Omega$ and $L = 6$ mH) for the tuning of the controllers. The following $\mathrm{PI_E}$ controller is obtained:

$$\mathrm{PI_E} = 0.7\frac{1 + 10^{-5}s}{s} \tag{20}$$

which has a bandwidth of 125 rad/s, a phase margin of 31.2 deg and a settling time of 0.098 s as depicted in Fig. 10.

The $\mathrm{PI}_{\mathrm{P}_m}$ controller is tuned according to the power balancing through the rotating inertia J of the SG in (10). By assuming small derivations from ω compared to ω_{nom}:

$$P_m - P = \omega_{\mathrm{nom}} J \frac{\mathrm{d}\omega}{\mathrm{dt}} \tag{21}$$

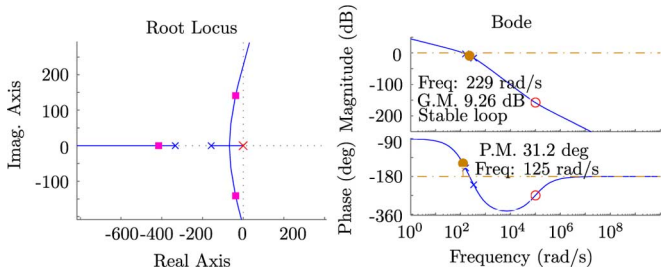

Fig. 10. Root Locus of the $\mathrm{PI_E}$ control loop.

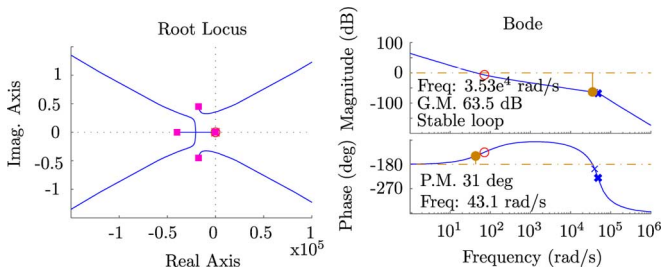

Fig. 11. Root Locus of the $\mathrm{PI_{P_m}}$ control loop.

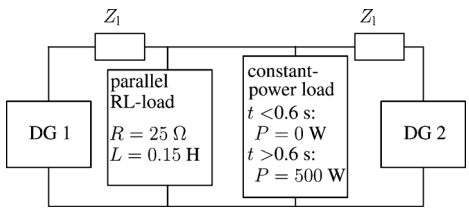

Fig. 12. Symmetrical microgrid, equally rated CIDG units.

with $\omega_{\mathrm{nom}} = 2\pi 50$ rad/s and $J = 0.18$ kgm^2. By using the Pade approximation P, the following $\mathrm{PI_{P_m}}$ controller is obtained:

$$\mathrm{PI_{P_m}} = 9 \cdot 10^4 \frac{1 + 0.014s}{s} \tag{22}$$

which has a bandwidth of 43.1 rad/s, a phase margin of 31 deg and a settling time of 0.377 s as depicted in Fig. 11. A sufficiently different phase margin between the $\mathrm{PI_E}$ and $\mathrm{PI_{P_m}}$ control loops is obtained.

C. Concept

A simulation in a basic microgrid is discussed as a proof of concept. Two units of equal ratings are included, either both CIDG units or one CIDG unit and one SG in a symmetrical microgrid with an RL load and a constant-power load are considered, with further details in Fig. 12.

1) Two CIDG Units: In this first simulation, two CIDG units with nominal active and reactive power of 1500 W and 0 VAr, respectively, and with equal droops are considered. Also, both DG units represent dispatchable units without constant-power band ($2b = 0$) and use the voltage-based droop control strategy. The simulations start from an rms terminal voltage of 230 V and a frequency of 50 Hz. The droop coefficients are: $k_d = -0.5$ V/V, $k_P = P_{\mathrm{nom}}/50$ W/V and $k_Q = f_{\max} - f_{\mathrm{nom}}/Q_{\max} = 5e^{-5}$ Hz/VAr.

The simulation results depicted in Fig. 13 show that no difference in P, V_{g}, Q and f between the DG units is obtained, because of their equal ratings, equal droops and the symmetrical microgrid. After 0.6 s, as the constant-power load turns on, both units increase their power identically. This increase is slightly less than 250 W each as also the grid voltage decreases, resulting in less consumption from the RL load. The simulations show that in steady-state: $P_1 = P_2 = 1318$ W, $V_{\mathrm{g},1} = V_{\mathrm{g},2} = 234.5$ V, $f_1 = f_2 = 50.016$ Hz and $Q_1 = Q_2 = 317$ VAr.

2) One CIDG Unit and an SG With Control Strategies Not Matched: In this simulation case, an SG is included instead of a CIDG unit. The SG is represented as an emf E in series with an inductance L of 6 mH. The SG uses conventional P/f and V_{g}/Q droop control and the CIDG unit uses the voltage-based droop control with $b = 0$.

In case of a high rotating inertia of the SG, $J = 18$ kgm^2, which is a high value for a small low-voltage connected unit, a stable operation can be reached. However, steady-state is slowly reached as shown in Fig. 14, mark the longer simulation time and the delayed load change in this figure. As in steady-state: $P_{\mathrm{CIDG}} = 1557.2$ W and $P_{\mathrm{SG}} = 937.1$ W, the power sharing is not according to the equal ratings of the units. In case the SG has a lower inertia J of 0.18 kgm^2, high power and voltage swings are obtained leading to an unstable operation opposed to the previous case where high inertia provides damping in the system.

3) One CIDG Unit and an SG With Control Strategies Matched: In this case, the control of the SG, with $J = 0.18$ kgm^2, uses converter behavior with P/V_{g} and Q/f droop control. Because the controllers are matched to each other, a stable operation is obtained, with equal ac-powers and terminal voltages, as depicted Fig. 15. In steady-state: $P_{\mathrm{CIDG}} = P_{\mathrm{SG}} = 1317$ W, $V_{\mathrm{g,CIDG}} = V_{\mathrm{g,SG}} = 234.4$ V, $Q_{\mathrm{CIDG}} = Q_{\mathrm{SG}} = 317$ VAr and $f_{\mathrm{CIDG}} = f_{\mathrm{SG}} = 50.016$ Hz.

Still, higher P, V_{g}, Q and f swings are present in the transients compared to the case of only CIDG units. These simulations show that implementing converter behavior in SGs can lead to adequate power sharing between SGs and CIDG units. It also enables to incorporate the SGs in a converter-based microgrid.

V. Synchronous Generator in the Microgrid

In this simulation example, a more extended microgrid is included as depicted in Fig. 16. One SG (with converter behavior) and three power-controlled CIDG units (with voltage-based droop controller) are included:

- G1 represents a fully dispatchable CIDG unit with $P_{\mathrm{dc1,nom}} = 1500$ W and $b = 0\%$.
- G2 represents an undispatchable CIDG unit (such as an intermittent renewable source) with $P_{\mathrm{dc2,nom}} = 500$ W. Only the $V_{\mathrm{g}}/V_{\mathrm{dc}}$ droop control is used as a large constant-power band $b = 20\%$, which is larger than the absolute grid voltage limits, is included. After 0.6 s, the primary energy source changes the dc power to $P_{\mathrm{dc2,nom}} = 4/3 \cdot 500$ W $= 667$ W.
- G3 represents a slightly dispatchable CIDG unit with $P_{\mathrm{dc3,nom}} = 1000$ W and $b = 5\%$.

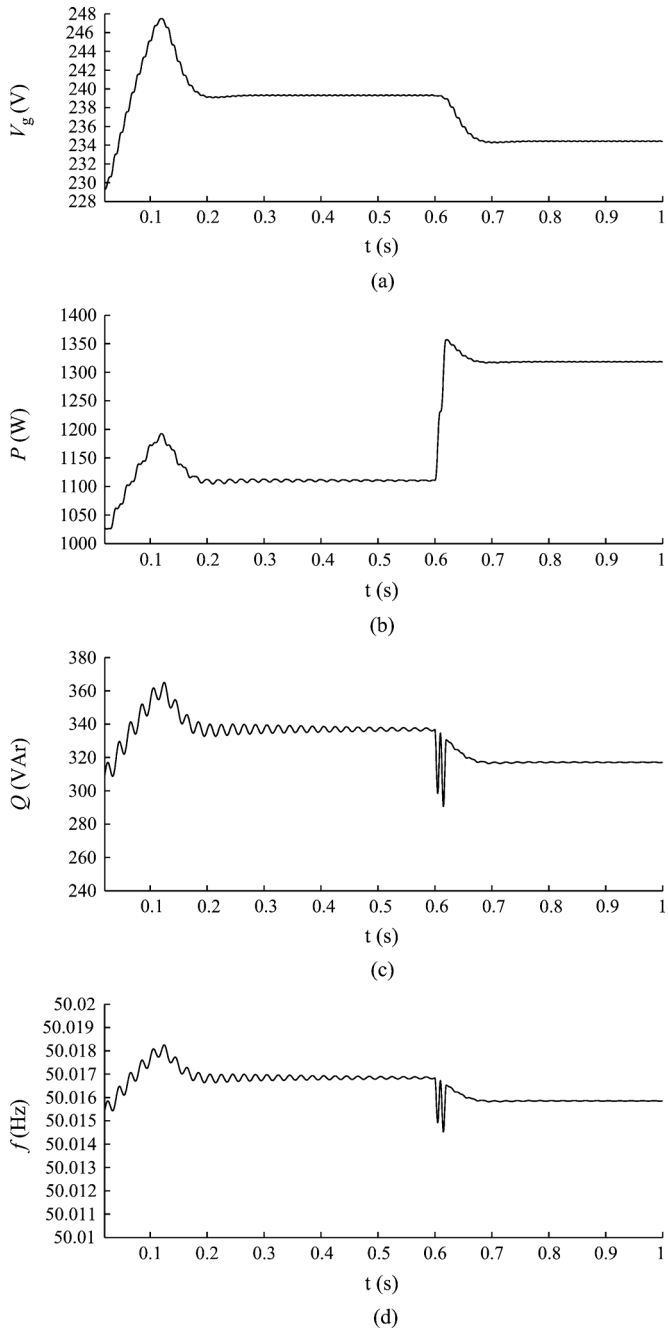

Fig. 13. Proof of concept: Symmetrical microgrid, equally rated CIDG units (— = CIDG 1; – – – = CIDG 2). (a) Microgrid voltage. (b) Active power to the electrical network. (c) Reactive power to the electrical network. (d) Microgrid frequency.

- The SG has nominal power 1500 W and is fully dispatchable.

One of the loads turns on after 0.45 s. The simulation results are depicted in Fig. 17.

The simulations show a stable operation. Also, the effect of the load change after 0.45 s and the generator change after 0.6 s are clearly visible. After the load change, the reaction of the SGs (change of P_m) is slower than that of the CIDG units. This simulation shows that the mechanical power P_m of the SG lags compared to the ac power, the difference between both leads to a change of angular speed of the SG. The PI controllers of the

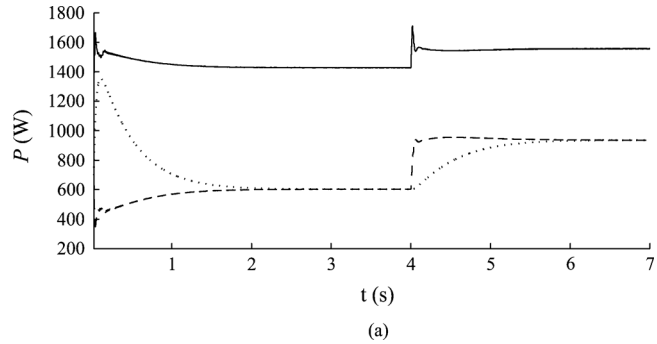

Fig. 14. Proof of concept: Symmetrical microgrid, CIDG unit and SG, control strategies not matched (— = CIDG; – – – = SG ac power, … = SG mechanical power). (a) Active power to the electrical network.

synchronous generator enable to use this generator in a resistive microgrid with voltage-based controllers of the CIDG units. G1 has the largest output power, and its $P_{\rm dc}/V_{\rm g}$ droop controller fully adjusts its output power to changes of the microgrid state. For example, at $t = 0.45$ s, when a load turns on, this generator significantly increases its output power. G2 on the other hand, has a constant output power, that is not determined by the microgrid state but by its prime energy mover. For example, at $t = 0.45$ s, the ac-power P increases, which is extracted from the dc-link capacitor because $P_{\rm dc,2}$ remains constant. Hence, the dc-link voltage of G2 decreases such that the $V_{\rm g}/V_{\rm dc}$ droop controller decreases $V_{\rm g}$ until a stable operation is obtained with $P = P_{\rm dc}$. The SG also adapts to the state of the microgrid and participates in the power sharing in the microgrid.

In steady-state, $P_1 = 2.18$ kW, $P_2 = 0.67$kW, $P_3 = 1.20$ kW and $P_{\rm SG} = 2.10$ kW. Therefore, good power sharing according to the ratings of the DG units (except for the undispatchable DG unit CIDG 2) is obtained. Some inaccuracies in power sharing can exist because of the line impedances as, opposed to frequency, the grid voltage is not a global parameter. These are however small because of the small line impedances in small-scale networks and because the voltage is controlled between strict voltage limits. However, secondary control can be used to further optimize the power sharing and voltage control [39]. The units deliver equal reactive power because of their equal droops and nominal values of Q.

VI. IEEE 13-Node Test Feeder

Also, a variant of the IEEE 13-Node Test Feeder in Fig. 18 is simulated. The IEEE 13-Node Test Feeder is modified for application as a low-voltage network in islanded mode. The simulation details of the nodes are summarized in Fig. 19, showing that a combination of various loads (resistive, inductive, constant-power and switching loads) is used. There are three CIDG units and two SGs connected to the feeder, with details summarized in Table I and with matched voltage-based droop controllers.

The current-controlled CIDG units use $I_{\rm dc}/V_{\rm g}$ droops with the resistive virtual output impedance $R_v = 3\ \Omega$ while the power-controlled CIDG unit has a $P_{\rm dc}/V_{\rm g}$ droop controller. The nominal dc-power of CIDG 1 and CIDG 3 can be calculated by taking into account R_v, and with $V_{\rm dc,nom} = 450$ V,

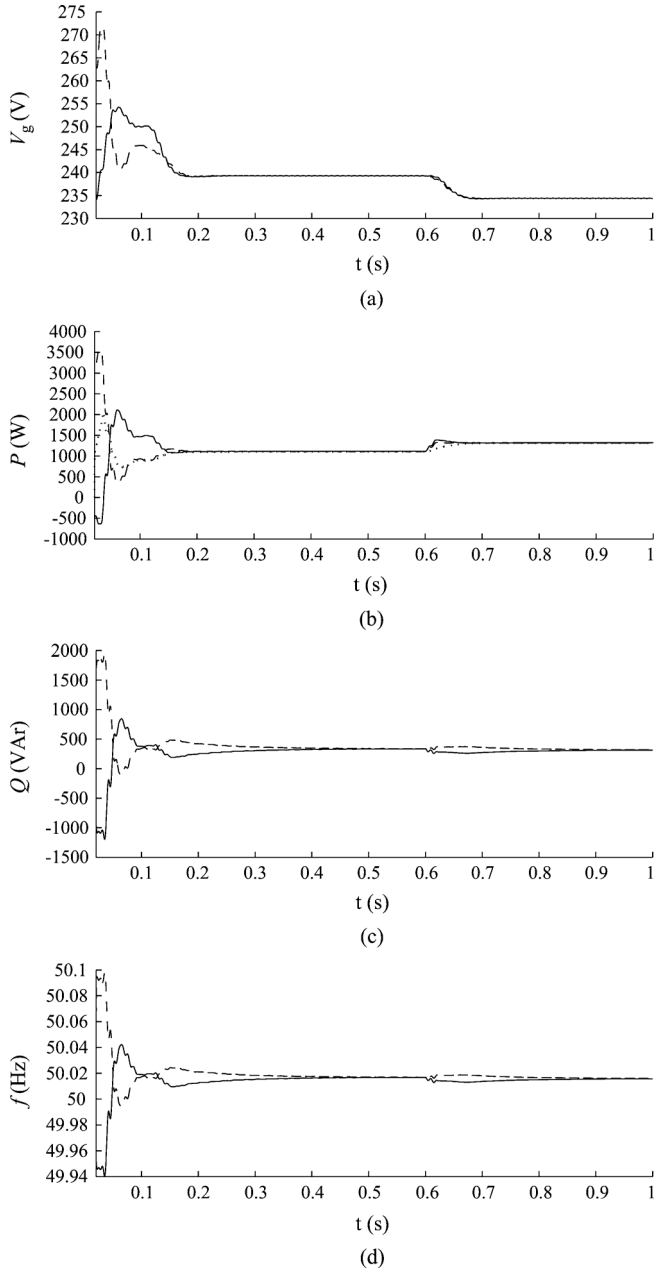

Fig. 15. Proof of concept: CIDG unit and SG, control strategies matched — = CIDG 1; – – – = SG). (a) Microgrid voltage. (b) Active power to the electrical network (— = CIDG 1; – – – = ac-power of SG, … = mechanical power of SG). (c) Reactive power to the electrical network. (d) Microgrid frequency.

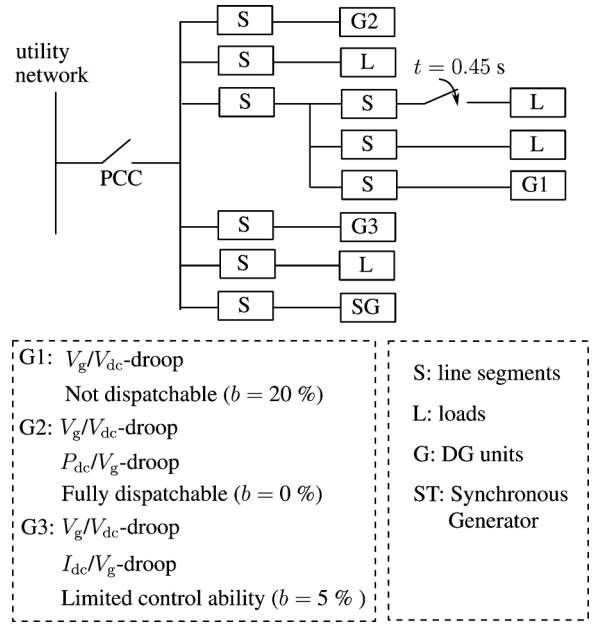

Fig. 16. Islanded microgrid including synchronous generator.

$k_d = 0.5$ and $V_{g,nom} = 230$ V. In nominal conditions: $P_{dc,nom,1} = 2.1$ kW, $P_{dc,nom,3} = 5.1$ kW in case $I_{dc,3} = 8$ A and $P_{dc,nom,3} = 3.0$ kW in case $I_{dc,3} = 5.3$ A.

In steady state, the simulation results in Fig. 20 give: $P_{CIDG1} = 1.9$ kW, $P_{CIDG2} = 3.5$ kW, $P_{CIDG3} = 3.0$ kW, $P_{SG1} = 4.3$ kW, $P_{SG2} = 3.5$ kW; and $I_{dc,CIDG1} = 3.6$ A, $I_{dc,CIDG2} = 7.7$ A and $I_{dc,CIDG3} = 5.3$ A. Hence, except for the undispatchable CIDG unit (voltage inside the constant-power band), power sharing according to the ratings of the units, for both the CIDG units and SGs, is obtained. Analogously, in steady-state all units deliver the same reactive power 757 VAr as their nominal Q and f, and thus, the droops are equal for all units. The figure also shows a clear delay in the changes of P_m compared to those of P. This delay is however restricted because of the small size of the SG. At $t = 0.5$ s, a resistive load turns of, which clearly results in a transient with decreasing power delivered by all DG units. At $t = 0.4$ s, the generation decrease from CIDG 3 is met by an increase in P of the other generators, both CIDG units and SGs.

In Fig. 21, the same case is studied, but the SGs have P/f and Q/V droop control instead of voltage-based droop control to emulate converter behavior. The steady-state results, e.g., of active power, show that the power sharing between the SGs and CIDG units is not according to the ratings: $P_{CIDG1} = 2.4$ kW, $P_{CIDG2} = 4.3$ kW, $P_{CIDG3} = 3.0$ kW, $P_{SG1} = 3.3$ kW, $P_{SG2} = 2.3$ kW. From this, it is concluded that in order to provide accurate power sharing, a match between the control strategies of SGs and CIDG units is required. Also, the reactive power sharing between SGs and CIDGs is not according to the ratings as the units have equal Q_{nom}, but the droops of the Q/f controller of the CIDG units and the P/f controllers of the SGs are not equal. Also, Δf and ΔV_g, namely the triggers to change P for the SGs and CIDG units, respectively, can differ. Compared to the case with matched control strategies, larger transients are obtained with consequent higher settling times.

VII. Conclusions

Because of an increasing share of DG units and the introduction of (islanded) microgrids, new control methods for the CIDG units in islanded microgrids are developed. In case of resistive microgrid lines, often, P/V_g droop controllers and a variant of this, namely voltage-based droop controllers, are used instead of the P/f droops that are based on the conventional grid control. However, still some SGs can be present in the microgrid, of which the P/f droop control does not comply with P/V_g droop control and the rotating inertia needs to be taken into account. Because SGs generally form the minor part of the generators in the microgrid, in this paper, the control strategy of the

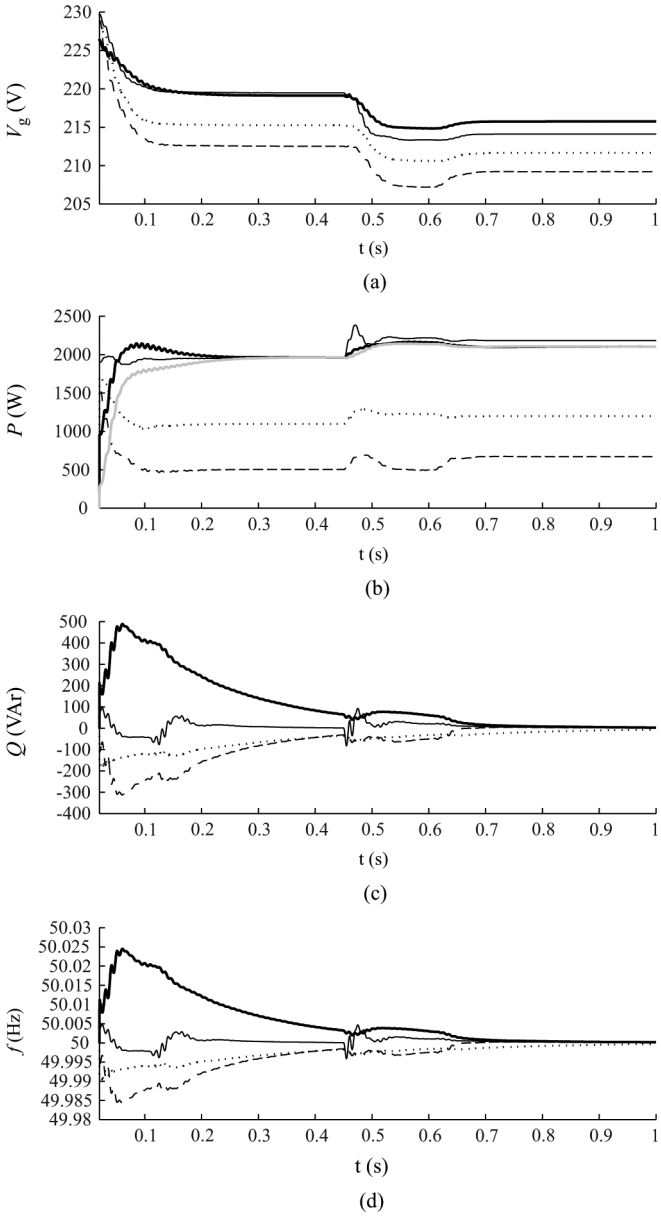

Fig. 17. SG in the microgrid (— = CIDG 1; – – – = CIDG 2, … = CIDG 3, — = SG, with ac-side power P in black and P_{m} in gray). (a) Microgrid voltage. (b) Active power to the electrical network. (c) Reactive power to the electrical network. (d) Microgrid frequency.

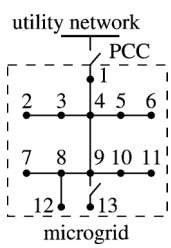

Fig. 18. IEEE 13-Node Test Feeder.

SGs is changed to comply with the CIDG unit control. This is implemented by including converter behavior in the SGs. The results show a stable operation of the islanded microgrid with a combination of SGs and CIDG units. The method also enables

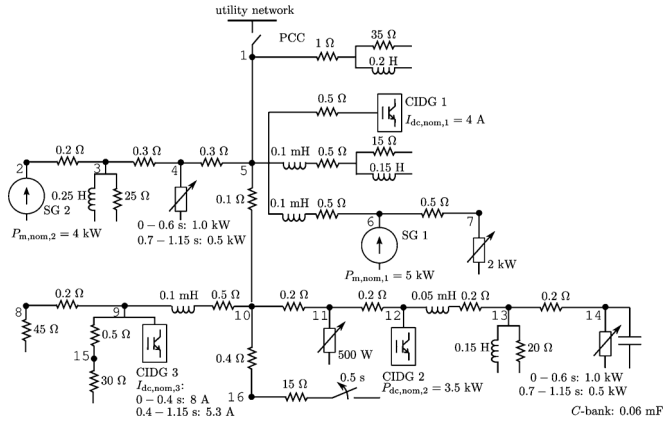

Fig. 19. 13-Node Test Feeder.

TABLE I
CIDG UNITS AND SGS IN TEST FEEDER: DETAIL

CIDG	dc-side -controlled	value	constant-power band
CIDG1	current	$I_{\mathrm{dc,nom},1} = 4$ A	$b = 0$ %
CIDG2	power	$P_{\mathrm{dc,nom},2} = 3.5$ kW	$b = 0$ %
CIDG3	current	$I_{\mathrm{dc,nom},3}$:	$b = 8$ %
		t <0.4 s: 8 A	
		t >0.4 s: 5.3 A	
SG1	power	$P_{\mathrm{m,nom},1} = 5$ kW	
SG2	power	$P_{\mathrm{m,nom},2} = 4$ kW	

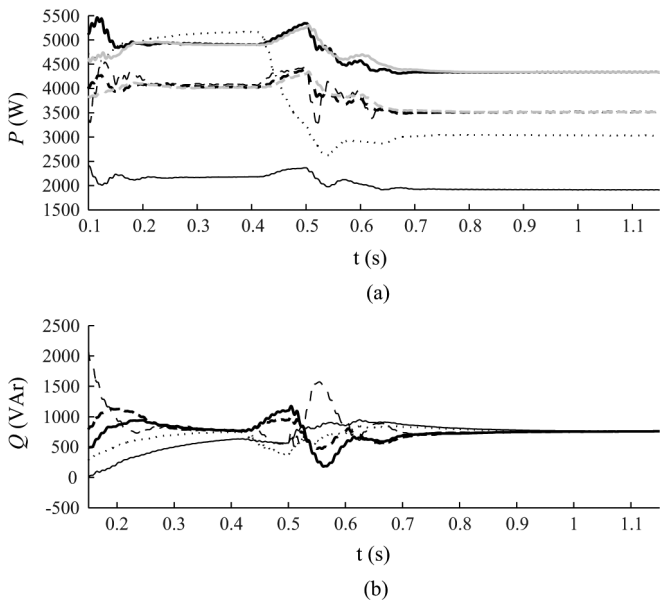

Fig. 20. 13-node test feeder (— = CIDG 1; ---- = CIDG 2, … = CIDG 3, — = SG1, ---- = SG2) (Extra in (a): — = SG1, ---- = SG2 with depending on the color: black = ac power and gray = mechanical power). (a) Active power to the network. (b) Reactive power to the network.

that both SGs and CIDG units can participate in accurate power sharing and balancing of islanded microgrids.

REFERENCES

[1] S. Barsali, M. Ceraolo, P. Pelacchi, and D. Poli, “Control techniques of dispersed generators to improve the continuity of electricity supply,” in *Proc. IEEE PES Winter Meeting*, 2002, pp. 789–794.

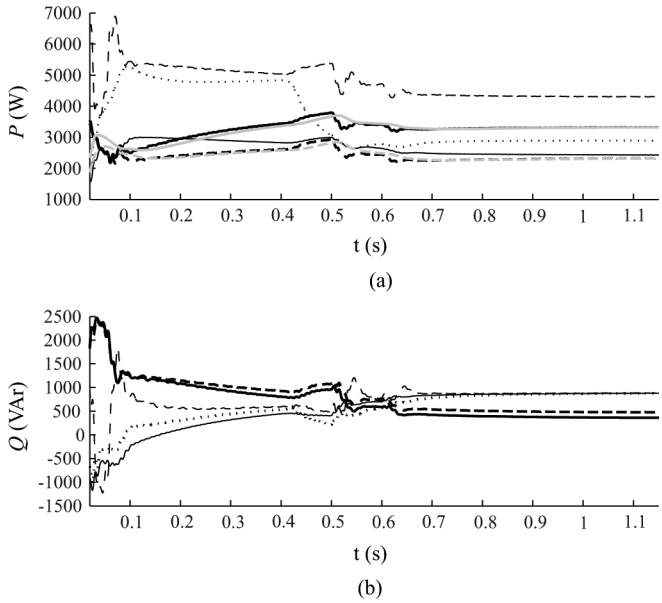

Fig. 21. 13-node test feeder with SGs using P/f and Q/V droop control (— = CIDG 1;---- = CIDG 2, ... = CIDG 3, — = SG1, ---- = SG2) (Extra in (a): — = SG1, ---- = SG2 with depending on the color: black = ac power and gray = mechanical power). (a) Active power to the network. (b) Reactive power to the network.

[2] R. H. Lasseter, A. Akhil, C. Marnay, J. Stephens, J. Dagle, R. Guttromson, A. Meliopoulous, R. Yinger, and J. Eto, The CERTS Microgrid Concept, White Paper on Integration of Distributed Energy Resources, California Energy Commission, Office of Power Technologies—U.S. Department of Energy, LBNL-50829, Apr. 2002. [Online]. Available: http://certs.lbl.gov.

[3] J. A. P. Lopes, C. Moreira, A. Madureira, F. Resende, P. G. Abia, X. Wu, N. Jayawarna, Y. Zhang, N. Jenkins, F. Kanellos, N. Hatziargyriou, and C. Duvauchelle, Microgrids Large Scale Integration of Microgeneration to low Voltage Grids: Dd1 Emergency Strategies and Algorithms, Oct. 2004. [Online]. Available: http://www.microgrids.eu/micro2000.

[4] A. Engler, O. Osika, M. Barnes, N. Jenkins, and A. Arulampalam, DB1 Local Micro Source Controller Strategies and Algorithms, European Commission, Feb. 2004. [Online]. Available: http://www.microgrids.eu/micro2000.

[5] N. Lidula and A. D. Rajapakse, "Microgrids research: A review of experimental microgrids and test systems," *Renew. Sustain. Energy Rev.*, vol. 15, no. 1, pp. 186–202, 2011.

[6] A. Mehrizi-Sani and R. Iravani, "Potential-function based control of a microgrid in islanded and grid-connected modes," *IEEE Trans. Power Syst.*, vol. 25, no. 4, pp. 1883–1891, Nov. 2010.

[7] H. Farhangi, "The path of the smart grid," *IEEE Power & Energy Mag.*, vol. 8, no. 1, pp. 18–28, Jan./Feb. 2010.

[8] A. G. Tsikalakis and N. D. Hatziargyriou, "Centralized control for optimizing microgrids operation," *IEEE Trans. Energy Convers.*, vol. 23, no. 1, pp. 241–248, Mar. 2008.

[9] C. Sao and P. Lehn, "Control and power management of converter fed microgrids," *IEEE Trans. Power Syst.*, vol. 23, no. 3, pp. 1088–1098, Aug. 2008.

[10] M. C. Chandorkar, D. M. Divan, and R. Adapa, "Control of parallel connected inverters in standalone ac supply systems," *IEEE Trans. Ind. Appl.*, vol. 29, no. 1, pp. 136–143, Jan./Feb. 1993.

[11] J. M. Guerrero, J. Matas, L. G. de Vicuña, M. Castilla, and J. Miret, "Wireless-control strategy for parallel operation of distributed-generation inverters," *IEEE Trans. Ind. Electron.*, vol. 53, no. 5, pp. 1461–1470, Oct. 2006.

[12] F. Katiraei and M. R. Iravani, "Power management strategies for a microgrid with multiple distributed generation units," *IEEE Trans. Power Syst.*, vol. 21, no. 4, pp. 1821–1831, Nov. 2006.

[13] R. H. Lasseter and P. Paigi, "Microgrid: A conceptual solution," in *Proc. IEEE Power Electron. Spec. Conf. (PESC 2004)*, Aachen, Germany, 2004.

[14] J. A. P. Lopes, C. L. Moreira, and A. G. Madureira, "Defining control strategies for microgrids in islanded operation," *IEEE Trans. Power Syst.*, vol. 21, no. 2, pp. 916–924, May 2006.

[15] W. Yao, M. Chen, J. M. Guerrero, and Z.-M. Qian, "Design and analysis of the droop control method for parallel inverters considering the impact of the complex impedance on the power sharing," *IEEE Trans. Ind. Electron.*, vol. 58, no. 2, pp. 576–588, Feb. 2011.

[16] H. Laaksonen, P. Saari, and R. Komulainen, "Voltage and frequency control of inverter based weak LV network microgrid," in *Proc. 2005 Int. Conf. Future Power Systems*, Amsterdam, The Netherlands, Nov. 18, 2005.

[17] A. Engler, O. Osika, M. Barnes, and N. Hatziargyriou, DB2 Evaluation of the Local Controller Strategies, Jan. 2005. [Online]. Available: http://www.microgrids.eu/micro2000.

[18] T. L. Vandoorn, B. Meersman, L. Degroote, B. Renders, and L. Vandevelde, "A control strategy for islanded microgrids with dc-link voltage control," *IEEE Trans. Power Del.*, vol. 26, no. 2, pp. 703–713, Apr. 2011.

[19] K. Visscher, Vsync—The Virtual Synchronous Generator Concept, Jul. 2008. [Online]. Available: http://www.vsycn.eu.

[20] Q.-C. Zhong and G. Weiss, "Synchronverters: Inverters that mimic synchronous generators," *IEEE Trans. Ind. Electron.*, vol. 58, no. 4, pp. 1259–1267, Apr. 2011.

[21] K. Siri, C. Q. Lee, and T. F. Wu, "Current distribution control for parallel connected converters part I," *IEEE Trans. Aerosp. Electron. Syst.*, vol. 28, no. 3, pp. 829–840, Jul. 1992.

[22] J.-F. Chen and C.-L. Chu, "Combination voltage-controlled and current-controlled PWM inverters for UPS parallel operation," *IEEE Trans. Ind. Electron.*, vol. 10, no. 5, pp. 547–558, Sep. 1995.

[23] K. Siri, C. Q. Lee, and T. F. Wu, "Current distribution control for parallel connected converters part II," *IEEE Trans. Aerosp. Electron. Syst.*, vol. 28, no. 3, pp. 841–851, Jul. 1992.

[24] J. Banda and K. Siri, "Improved central-limit control for parallel-operation of dc-dc power converters," in *Proc. IEEE Power Electronics Specialists Conf. (PESC '95)*, Atlanta, GA, Jun. 18–22, 1995, pp. 1104–1110.

[25] M. Marwali, J.-W. Jung, and A. Keyhani, "Control of distributed generation systems—part II: Load sharing control," *IEEE Trans. Power Electron.*, vol. 19, no. 6, pp. 1551–1561, Nov. 2004.

[26] F. Katiraei, R. Iravani, N. Hatziargyriou, and A. Dimeas, "Microgrids management: Controls and operation aspects of microgrids," *Power & Energy Mag.*, vol. 6, no. 3, pp. 54–65, May/Jun. 2008.

[27] K. Debrabandere, B. Bolsens, J. Van den Keybus, A. Woyte, J. Driesen, and R. Belmans, "A voltage and frequency droop control method for parallel inverters," *IEEE Trans. Power Electron.*, vol. 22, no. 4, pp. 1107–1115, Jul. 2007.

[28] F. A. Bhuiyan and A. Yazdani, "Multimode control of a DFIG-based wind-power unit for remote applications," *IEEE Trans. Power Del.*, vol. 24, no. 4, pp. 2079–2089, Oct. 2009.

[29] A. Engler, "Applicability of droops in low voltage grids," *DER J.*, no. 1, Jan. 2005.

[30] J. M. Guerrero, J. Matas, L. García de Vicuña, M. Castilla, and J. Miret, "Decentralized control for parallel operation of distributed generation inverters using resistive output impedance," *IEEE Trans. Ind. Electron.*, vol. 54, no. 2, pp. 994–1004, Apr. 2007.

[31] J. M. Guerrero, J. C. Vásquez, J. Matas, M. Castilla, and L. García de Vicuña, "Control strategy for flexible microgrid based on parallel line-interactive UPS systems," *IEEE Trans. Ind. Electron.*, vol. 56, no. 3, pp. 726–736, Mar. 2009.

[32] J. Matas, L. G. de Vicuña, and J. C. Vasquez, "Virtual impedance loop for droop-controlled single-phase parallel inverters using a second order general integrator scheme," *IEEE Trans. Power Electron.*, vol. 25, no. 12, p. 2993, Dec. 2010.

[33] Y. Li and Y. W. Li, "Power management of inverter interfaced autonomous microgrid based on virtual frequency-voltage frame," *IEEE Trans. Smart Grid*, vol. 2, no. 1, pp. 30–40, Mar. 2011.

[34] J. M. Guerrero, L. García de Vicuña, J. Matas, M. Castilla, and J. Miret, "Output impedance design of parallel-connected ups inverters with wireless load-sharing control," *IEEE Trans. Ind. Electron.*, vol. 52, no. 4, pp. 1126–1135, Aug. 2005.

[35] J. Driesen and K. Visscher, "Virtual synchronous generators," in *Proc. IEEE PES General Meeting*, Pittsburgh, PA, Jul. 20–24, 2008.

[36] M. Prodanovic and T. C. Green, "High-quality power generation through distributed control of a power park microgrid," *IEEE Trans. Ind. Electron.*, vol. 53, no. 5, pp. 1471–1482, Oct. 2006.

[37] A. Tuladhar, H. Jin, T. Unger, and K. Mauch, "Control of parallel inverters in distributed AC power systems with consideration of line impedance effect," *IEEE Trans. Ind. Appl.*, vol. 36, no. 1, pp. 131–138, Jan./Feb. 2000.

[38] K. S. Parlak, M.Özdemir, and M. T. Aydemir, "Active and reactive power sharing and frequency restoration in a distributed power system consisting of two ups units," *Elect. Power Energy Syst.*, vol. 31, no. 5, pp. 220–226, Jun. 2009.

[39] J. M. Guerrero, J. C. Vásquez, J. Matas, L. Garcí de Vicuña, and M. Castilla, "Hierarchical control of droop-controlled AC and DC microgrids—A general approach towards standardization," *IEEE Trans. Ind. Electron.*, vol. 58, no. 1, pp. 158–172, Jan. 2011.

Tine L. Vandoorn (S'09) was born in Torhout, Belgium, in 1985. She received the M.S. degree in electromechanical engineering from Ghent University, Ghent, Belgium, in 2008, where she is currently pursuing the Ph.D. degree.

In 2008, she joined the Electrical Energy Laboratory (EELAB) of Ghent University. Her present research interests include electric power systems, voltage and power control of DG units, management of microgrids and smart microgrids. In 2009, she was awarded a grant as Ph.D. fellow of the Research Foundation Flanders (FWO).

Bart Meersman (S'07) was born in Sint-Niklaas, Belgium, on July 29, 1983. He received the M.S. degree in electromechanical engineering from Ghent University, Ghent, Belgium, in 2006, where he is currently pursuing the Ph.D. degree.

Since then, he has been with the Electrical Energy Laboratory (EELAB) of Ghent University. His present research interests include dynamic phasors, renewable energy applications, digital control of power electronic converters and their contribution to power quality.

Jeroen D. M. De Kooning (S'09) was born in Kapellen, Belgium, in 1987. He received the M.S. degree in electromechanical engineering from Ghent University, Ghent, Belgium, in 2010,, where he is currently pursuing the Ph.D. degree.

Since then, he has been with the Electrical Energy Laboratory (EELAB) of Ghent University. His present research interests include wind energy systems and control of power electronic converters.

Lieven Vandevelde (M'05-SM'07) was born in Eeklo, Belgium, in 1968. He received the M.S. degree in electromechanical engineering and the Ph.D. degree from Ghent University, Ghent, Belgium, in 1992 and 1997, respectively.

He is with the Electrical Energy Laboratory (EELAB), Ghent University, where he has been a Professor in electrical power engineering since 2004. His research and teaching activities are in the field of electric power systems, electrical machines and (computational) electromagnetics.